

Corrosion Behaviour of Co-Cr Dental Alloys Processed by Alternative CAD/CAM Technologies in Artificial Saliva Solutions

Cristina E Savencu^{1,*}, *Liviu V Costea*², *Mircea L Dan*², *Liliana Porojan*¹

¹ Department of Dental Prostheses Technology, School of Dentistry, University of Medicine and Pharmacy V. Babeş, Timișoara, Romania

² Faculty of Industrial Chemistry and Environmental Engineering, Politehnica University of Timișoara, Romania

*E-mail: cristina.savencu@umft.ro

Received: 18 November 2017 / *Accepted:* 30 January 2018 / *Published:* 6 March 2018

The purpose of this study was to evaluate the corrosion behaviour of cobalt-chromium dental alloys processed by alternative computer assisted technologies compared to conventional casting technology. Samples obtained by CAD/CAM milling (MIL), Selective Laser Sintering (SLS), Selective Laser Melting (SLM) and conventional melting- casting technology (CAS) were subjected to different electrochemical techniques: linear polarization (LV), cyclic voltammetry (CV), electrochemical impedance spectroscopy (EIS) and chronochemical studies (chronoamperometry - CA and chronopotentiometry - CP). These methods have been successfully employed in the investigation of various corrosion processes in the field of dentistry. The corrosive electrolyte used for the electrochemical tests was Fusayama artificial saliva with pH values of 5.5, close to the physiological value. The temperature was kept constant at 37°C. The samples were analysed by scanning electron microscopy (SEM) before and after performing corrosion testing. Computer assisted processing technologies showed promising results, representing a good alternative to traditional manufacturing methods for metallic frameworks for dental prostheses.

Keywords: corrosion resistance, electrochemical behaviour, Selective Laser Sintering, Selective Laser Melting, dental alloy milling, biomaterials, metal casting

1. INTRODUCTION

Base alloys such as cobalt-chromium alloys have been successfully used in medicine since 19th century, replacing noble alloys in dentistry [1], and are still widely used in the manufacturing of frameworks for fixed or removable partial restorations traditionally produced using the conventional melting-casting technology. New alternative methods, such as computer-aided design/computer-aided

manufacturing (CAD/CAM) subtractive and additive technologies have managed, in recent years, to make the transition from industry towards dental technology [2].

Electro-chemical degradation is the most important phenomenon that affects metallic restorations in the oral cavity [3]. Corrosion products may affect the biocompatibility of the employed alloys due to the release of metal ions, which may lead to local reactions such as discoloration, inflammation of surrounding tissue or systemic reactions, namely allergic reactions [4, 5, 6]. Mechanical properties, as well as clinical performances of the used alloys could thus also be impaired [7, 8].

Being mounted in the oral cavity, dental alloys are subjected to a wet environment, getting in contact with various types of ions and undergoing pH and/or temperature changes, mechanical as well as electrochemical wear which in the end may lead to corrosion phenomena. The electrochemical degradation of dental alloys can be triggered by a number of factors, such as chemical composition, microstructure, manufacturing method as well as surface processing [9]. Environmentally occurring oxygen may interact with the metal surface by forming an oxide layer which could act as a barrier, protecting the base alloy against further corrosive attack. The oxide layer can be dissolved when the breakdown potential of the alloy is reached, leaving the alloy surface exposed, hence more susceptible to undergoing corrosion [10].

Furthermore, corrosion products that could be generated by Co-Cr alloys possess cytotoxic, genotoxic and metal sensitizing effects [5]. Considering the fact that different processing techniques often lead to different metal microstructures and that alternative computer assisted technologies are used in dental field for a short period of time, the corrosion behaviour of the alloys should be studied in detail, to evaluate their biocompatibility [11].

The present study is aiming to compare the corrosion behaviour of metal frameworks manufactured out of Co-Cr alloys processed by various computer assisted technologies as alternatives to traditional casting techniques.

2. MATERIALS AND METHODS

Four groups of disk-shaped samples with a diameter of 10 mm and 2 mm thickness were produced by melting-casting (CAS) using a commercial Co-Cr base material, CAD/CAM milling (MIL) using prefabricated Co-Cr dental alloy blocks, selective laser melting (SLM) and selective laser sintering (SLS) using Co-Cr powder. The chemical composition of the investigated probes, as given by the manufacturer, is detailed in Table 1. The samples employed in the CAS technique were made from wax, invested and casted using a vacuum pressure casting machine. The samples were divested after cooling down, air-blasted with alumina particles and mechanically finished and polished using specific instruments.

MIL samples were obtained using a 5 axis milling machine from a prefabricated block of type 4 Co-Cr dental alloy. A type 4 Co-Cr powder alloy was used to prepare metallic plates by the SLS and SLM techniques respectively. Relief-firing under argon was conducted up to 450°C within 60 minutes, holding for 45 minutes, for additive manufactured samples.

Oxide-firing (at 950 – 980°C) was performed, as required for porcelain veneering for all samples, the metal surface was blasted with fresh aluminum oxide (75 µm). All samples were finished furthermore with wet silicon carbide sheets and 1µm grit diamond paste respectively, degreased in ethanol and finally sonicated in distilled water, rinsed and dried prior to performing electrochemical investigations.

The surface morphology has been investigated by scanning electron microscopy (SEM) using a FEI INSPECT S microscope before and after conducting the corrosion tests.

Table 1. Composition of analysed dental alloys (expressed as percentage by weight)

Probe	Co	Cr	Mo	Mn	W	Si	Fe	C
CAS	61.5	26	6	<1	5	<1	<1	0
MIL	61	28	0	0.25	8.5	1.65	<0.5	<0.1
SLS	59	25	3.5	<1.5	9.5	<1	<1.5	<1.5
SLM	59	25	3.5	<1.5	9.5	<1	<1.5	<1.5

Several electrochemical techniques were employed to accurately evaluate the corrosion mechanisms that occur in Co-Cr alloys exposed to the simulated physiological environment: linear polarization (LV), cyclic voltammetry (CV), electrochemical impedance spectroscopy (EIS), chronochemical studies (chronoamperometry - CA and chronopotentiometry - CP). Electrochemical investigations have been undertaken using a BioLogic SP150 potentiostat/ galvanostat along with a conventional three-electrode cell system. The mentioned testing methods have been used to assess corrosion processes in dentistry, according to ISO 10271 [12]. The electrolyte solution used during the electrochemical tests was a Fusayama artificial saliva solution [13] with pH of 5.5, at 37°C constant temperature (Table 2).

Table 2. Composition of the employed artificial saliva (modified Fusayama formulation, [13]):

Component	Concentration [g.L ⁻¹]
NaCl	0,4
KCl	0,4
CaCl ₂ .2H ₂ O	0,795
NaH ₂ PO ₄ .H ₂ O	0,690
Na ₂ S.9H ₂ O	0,005
Urea	1,0
KSCN	0,3

The investigated metal alloys were successively used as working electrodes. The counter electrodes consisted of two graphite rods, and Ag/AgCl acted as reference electrode. All potentials are referred to the saturated Ag/AgCl reference electrode ($E_{Ag/AgCl} = 0.197$ V/NHE).

Electrochemical impedance spectroscopy (EIS) investigations have been conducted using a BioLogic SP150 potentiostat/galvanostat equipped with an EIS module, within the frequency between 100 kHz and 10 MHz the amplitude of the alternating voltage was of 10 mV. A number of 60 points have been recorded for each spectrum with a logarithmic distribution of 10 points per decade. The experimental data has been fitted using the ZView – Scribner Associates Inc. software and equivalent electrical circuits by applying the Levenberg – Marquardt least squares complex non-linear fitting algorithm.

3. RESULTS AND DISCUSSION

Metal ion release within saliva is an important issue with respect to the biocompatibility as well as long-term toxicity potential of metallic prostheses [14, 15]. Since most corrosion phenomena occur through electrochemical transformations located at the interface between the metallic surface and electrolyte solution, most of the parameters describing the latter transformation are obtained by employing specific electrochemical methods.

The variation of the open circuit potential (OCP) over time for the materials investigated using artificial saliva as corrosion medium, is shown in Figure 1. Physically dissolved atmospheric oxygen has not been removed from the electrolyte solution prior to the testing in order to simulate conditions found in the oral cavity.

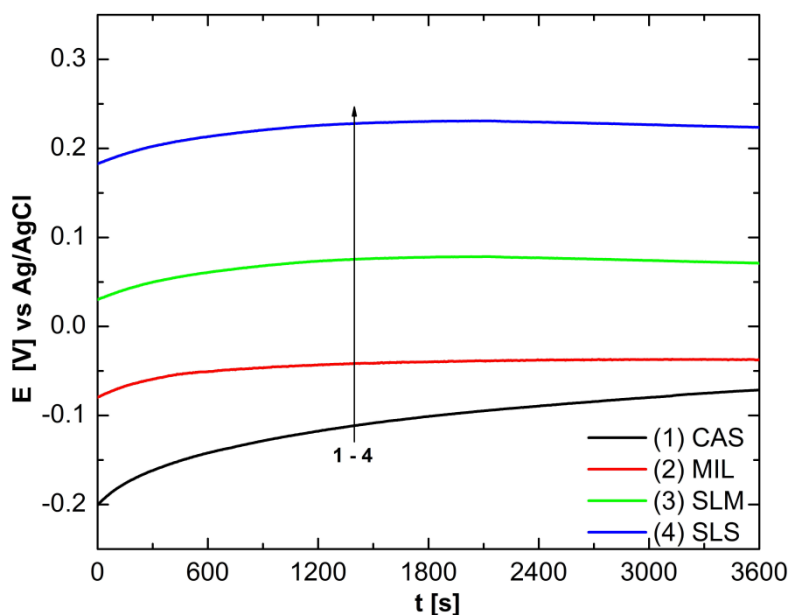


Figure 1. Evolution of the open circuit potential over time for the investigated samples in artificial saliva at 37°C.

Measuring the potential variation of the studied alloys acting as working electrodes over time provides information regarding the stability of the metallic compounds towards the electrolyte in

which they are immersed as well as a preliminary evaluation of the corrosion potential. A certain shift towards positive potentials (ennoblement) is observed in all four samples in the first 600 seconds, probably due to the formation of a protective film on the alloy surface. This behaviour is in accordance with the literature data [16,17]. The ennoblement region is rapidly followed by potential stabilization probably caused by the thickening of the protective film coating. The similar shapes of the OCP variation may be attributed to the presence of Cr within the studied alloys [18]. The CAS sample exhibits a different behaviour showing a steady increase in potential over the whole timescale, hence a greater tendency towards corrosion. All the samples show stabilized OCP potentials (E_{OCP}) within the region of -0.1 - +0.22 V vs. ref with the most positive potential being recorded for the SLS sample.

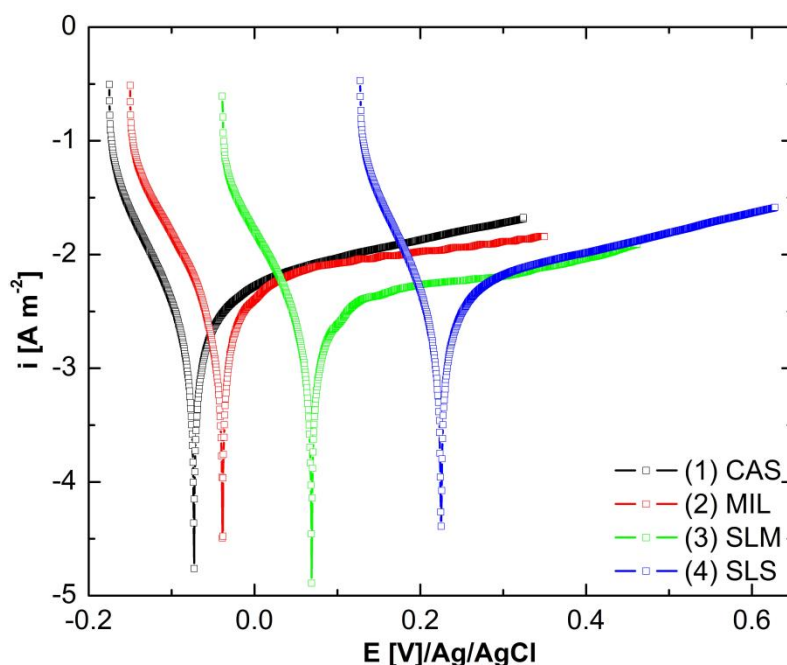


Figure 2. Tafel polarization curves for the studied samples in artificial saliva, at 37°C and a scan rate of 1 mV·s⁻¹

The variation of the logarithm of the current density with electrode potential recorded for all of the studied samples exposed to the Fusayama artificial saliva are illustrated comparatively in Figure 2. The obtained dependencies have been adapted using the Bio-Logic EC-Lab[®] software package, in order to determine the corrosion specific parameters for each of the four tested samples. The corrosion current density (i_{corr}), corrosion potential (E_{corr}), cathodic and anodic Tafel slopes (b_c and b_a), polarization resistance (R_p) and corrosion rate (v_{corr}) respectively, are listed in Table 3. All samples exhibit very similar corrosion behaviour. The cathode region of the potentiodynamic curves reveals a sudden current increase, suggesting either H⁺ or O₂ reduction, the latter being more likely to occur since no deaeration of the electrolyte solution was performed prior to the electrochemical measurements. Scanning towards anodic potentials reveals a passivating region, common to almost all studied samples in accordance to the literature data [19, 20]. A relatively slow but steady current

increase can be seen in the CAS as well as in the SLS samples, indicating a possible pseudo-passivation process probably due to a non-homogenous surface structure limiting the formation of a protective oxide layer.

Table 3. Corrosion parameter data for the investigated dental alloys in artificial saliva

Sample	i_{corr} [$\mu\text{A cm}^{-2}$]	E_{corr} [mV]	$-b_c$ [mV dec ⁻¹]	b_a [mV dec ⁻¹]	R_p [k Ω]	$v_{corr} 10^3$ [mm year ⁻¹]
CAS	0.208	-71	124	54.7	62.6	2.84
MIL	0.248	-38.7	141	69.8	60.5	3.20
SLM	0.356	71.4	145	71.4	45.5	4.46
SLS	0.379	223	132	62.1	36.8	4.97

Cyclic voltammetry was employed in order to further investigate the electrochemical behaviour of the studied samples. The potentiodynamic measurements recorded at a scan speed of 100 mV s⁻¹ covered a wide potential window reaching from a cathode potential of about -1.2 V vs. ref. in the Hydrogen evolution area, to an anodic polarization of 1.0 V vs. ref. where the release of metal ions from the electrode material is likely to occur. A comparative view of the obtained dependencies for the four alloys is shown in Figure 3.

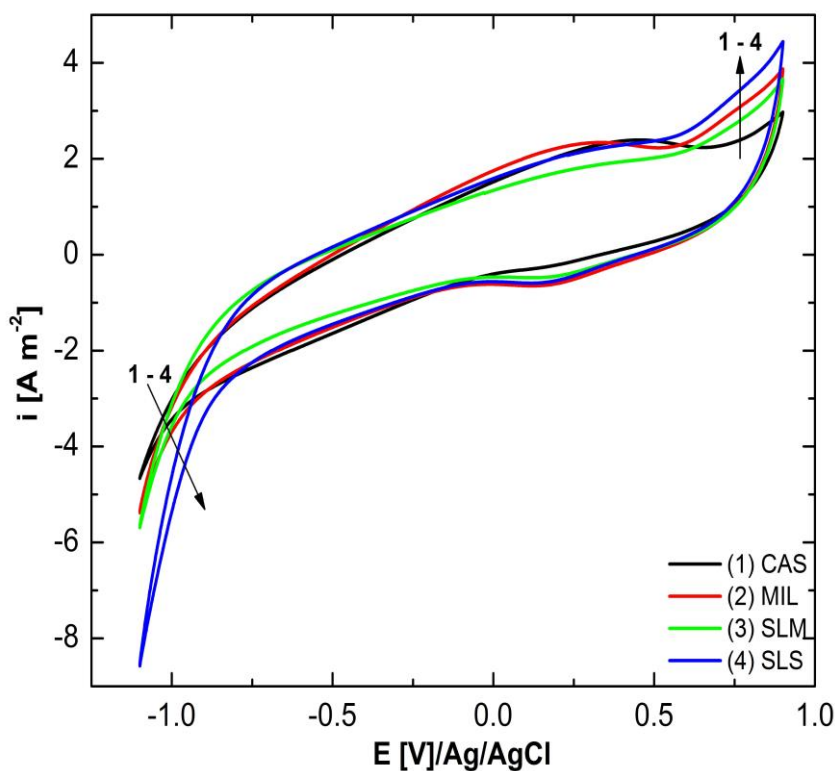


Figure 3. Cyclic voltammograms recorded on the studied dental alloys samples in artificial saliva at 37°C and a scan rate of 100 mV·s⁻¹

The potential has been varied starting from the previously determined E_{OCP} towards more positive potentials until the oxygen evolution process became detectable. The cathodic limit has been set by the hydrogen evolution reaction. All investigated samples show a relatively large passivation region, this finding being reported by other authors as well [21]. Scanning towards anodic regions reveals a relatively sharp current increase starting at a potential of about +0.5 V vs. ref. for CAS, MIL and SLM probes whereas SLS probe exhibiting a more stable behaviour, with a lower increase in current density occurring only at about +0.75 V vs. ref. This variation can be attributed to a greater stability towards metal dissolution of SLS sample due to a relatively compact oxidative film forming and growing steadily on the surface. The CAS, MIL and SLM samples show similar anodic shapes characterized by swift increases of the current at potentials more positive than +0.5 V, reflecting either a highly porous or weakly adhering oxide layer on the metal surface. CAS and MIL probes show a couple of linked broad peaks situated at $E_{pa} = +0.48$ V and $E_{pc} = +0.2$ V, at a potential difference characteristic for a quasireversible electrode process [22]. A similar cathodic peak has been recorded for the SLM sample as well, but without the occurrence of its anodic counterpart. This signal could have been caused by the dissolution of the passivating film formed during the anodic scan. Scanning towards more negative potentials reveals a sharp current increase in the case of the SLS probe, possibly due to the hydrogen evolution reaction. All other samples show a much lower current density in that region, indicating a higher resistance towards electrochemical corrosion in artificial saliva. Summarizing, we can observe that the CAS sample is exhibiting the most stable behaviour towards corrosion in the given medium with a large passivating area characterized by the lack of any anodic signals.

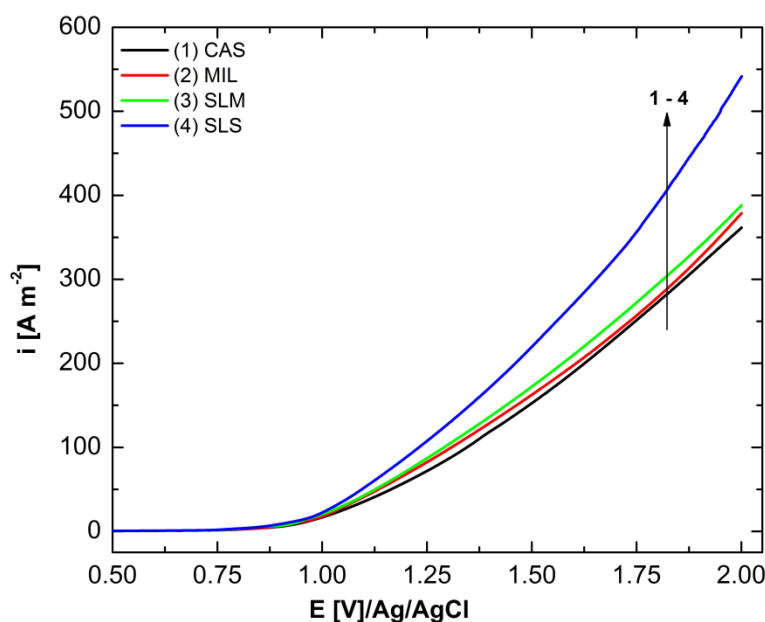


Figure 4. Linear voltammograms recorded for the studied samples in artificial saliva at 37°C and a scan rate of $10 \text{ mV} \cdot \text{s}^{-1}$

Linear polarization curves have been recorded for all four studied samples in artificial saliva (Figure 4) starting from the open circuit potential towards more positive potentials in order to identify

the oxidation processes that may occur at the electrode surface. The recorded polarization curves of the anodic region for the studied samples come to confirm the behaviour shown previously, namely the steady increase of the current density starting at a potential of about 0.85 V vs. ref. due to the oxygen evolution reaction. The lack of any oxidation signal within the studied potential region confirms that the current passing through the electrode/electrolyte interface does not trigger the ionization of the metals from the investigated alloys. The highest overall rate of oxygen evolution is recorded on the SLS probe, while the CAS sample accounts for the lowest current density in the potential region between 0.85 - 2.0 V vs. ref., the latter specimen being the most stable towards corrosion in the studied electrolyte. None of the examined specimens exhibit distinctive peaks due to metal dissolution, most probable due to an adherent and continuous protective oxide layer formed on the surface.

The electrochemical impedance spectra have been recorded in order to investigate the corrosion processes occurring on the surface at the corresponding corrosion potentials (E_{corr}). The obtained results are shown in Figure 5 as Nyquist and Bode plots respectively.

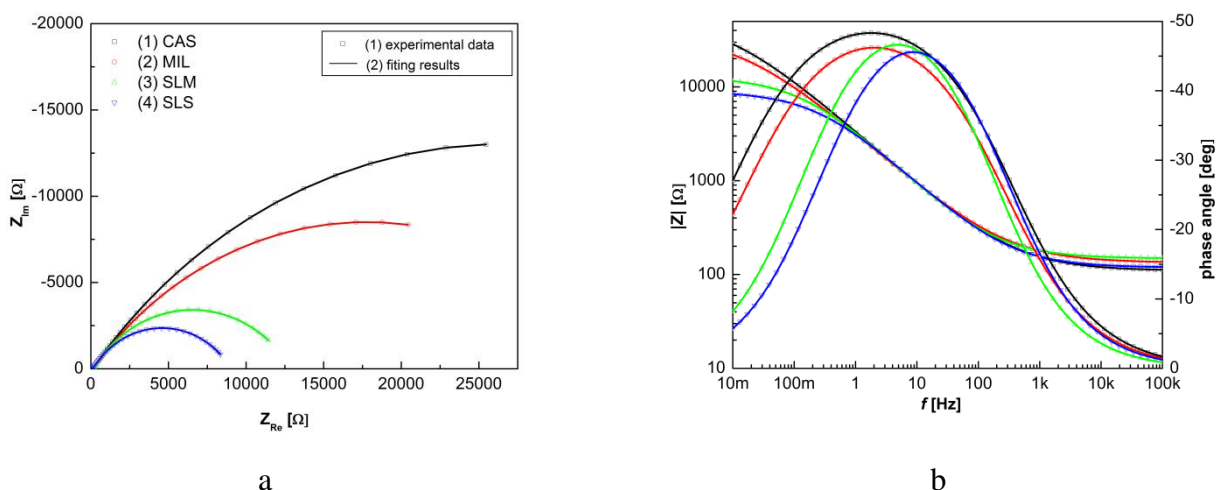


Figure 5. Nyquist (a) and Bode plots (b) recorded at corrosion potentials on tested dental alloys samples in artificial saliva at 37°C.

EIS data has been fitted using a complex non-linear least squares (CNLS) procedure with the equivalent electrical circuits (EEC) shown in Figure 6 [23].

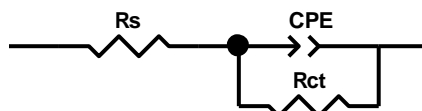


Figure 6. Equivalent circuit used for modelling corrosion process of the tested dental alloys in artificial saliva.

The EEC consists in a solution resistance R_s in series with a parallel connection of the charge transfer resistance R_{ct} and a constant phase element (CPE). R_s represents the uncompensated solution resistance. The ideal capacitor characterized by the double layer capacity (C_{dl}) is usually replaced by a constant phase element (CPE) because it more precisely represents the real electrochemical behaviour of the studied systems. The impedance of the CPE element is described by the Eq. E1:

$$ZCPE = 1/T(j\omega)^n \tag{E1}$$

where T is a parameter proportional with the double layer capacity, n is an exponent ranged between 0 and 1 which describes CPE angle.

The fitting results are depicted as continuous lines in Figure 5 and the obtained values of the circuit elements are given in Table 4 for the corrosion process of the investigated dental alloys in artificial saliva electrolyte. The values for the double layer capacity have been calculated as well.

Table 4. Calculated values of the EES elements on dental alloys samples in artificial saliva electrolyte

Sample	E [mV]	Rs [Ω cm ²]	T · 10 ⁵ [F cm ⁻² s ⁿ⁻¹]	n	Rct [kΩ cm ²]	Cdl · 10 ⁴ [F cm ⁻²]	Chi ² · 10 ³
CAS	-71.87	109.7 (1.3%)	10.2 (2.9%)	0.58 (1.3%)	53.01 (2.5%)	3.38	2.72
MIL	-38.72	133.7 (1.6%)	10.1 (2.3%)	0.59 (0.9%)	35.24 (2.3%)	2.70	1.32
SLM	71.4	148.2 (1.2%)	8.56 (1.3%)	0.62 (0.9%)	12.78 (2.2%)	0.90	1.16
SLS	222.7	118.4 (0.9)	8.23 (1.8%)	0.61 (0.6%)	8.94 (1.4%)	0.68	0.56

The interfacial double-layer capacitance (C_{dl}) values have been estimated using equation E2:

$$Cdl = T \cdot 1 / n \left(\frac{1}{R_s} - \frac{1}{R_{ct}} \right)^{\frac{n-1}{n}} \tag{E2}$$

The diameter of the semicircle is directly proportional to the charge transfer resistance (R_{ct}) and the corrosion rate of the investigated samples. The charge transfer resistances are large, of the order of kΩ, which is an indication for a high corrosion resistance of the studied alloys. The corrosion resistance of the alloy is proportional to the value of the transfer charge resistance. The occurrence of a single semicircle on the Nyquist diagrams in Figure 5 confirms that the mechanism of the electrode process is identical for all 4 analysed samples. It also suggests that at the interface between the dental alloys and artificial saliva a only single process takes place, namely the ionisation of the metals along with the formation of metallic oxides, adherent to the surface. This assumption is further confirmed by SEM images. The magnitude of the double layer capacity (C_{dl}) decreases with the decrease of the charge transfer resistance, which confirms the proposed mechanism of the studied electrode process. The EIS data come to confirm the previously detailed results from linear polarization studies, with best corrosion-resistance found for the alloy manufactured through the CAD milling technique.

In order to further elucidate the comparative corrosion behaviour of the studied samples, chronoamperometric determinations have been recorded in which the applied constant overpotential of +250 mV vs. E_{Corr} for each probe generated a variable current flow, the latter being recorded over a period of 15 minutes (Fig. 7). A common feature of all four studied samples is the rapid decrease of the current density, followed by its stabilization after about 5 minutes, probably due to the formation and growth of a passive oxide film and a consequent increase in interfacial resistance, as suggested by the literature [24]. All the samples exhibit similar slopes of the constant current region, suggesting resemblant corrosion mechanisms, however, greater currents have been recorded for the alloys manufactured by the SLS and the SLM technique compared to those obtained by the MIL and CAS procedures.

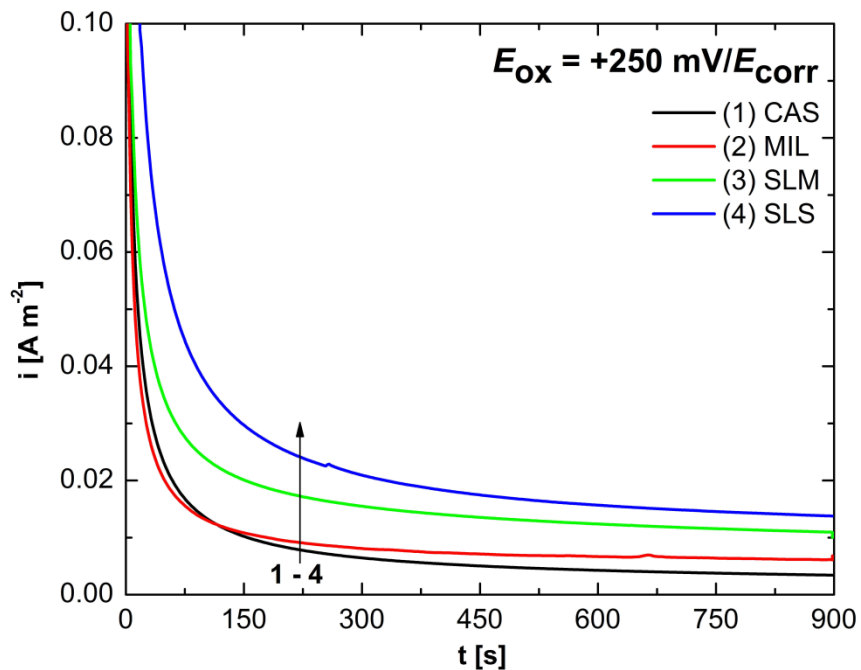
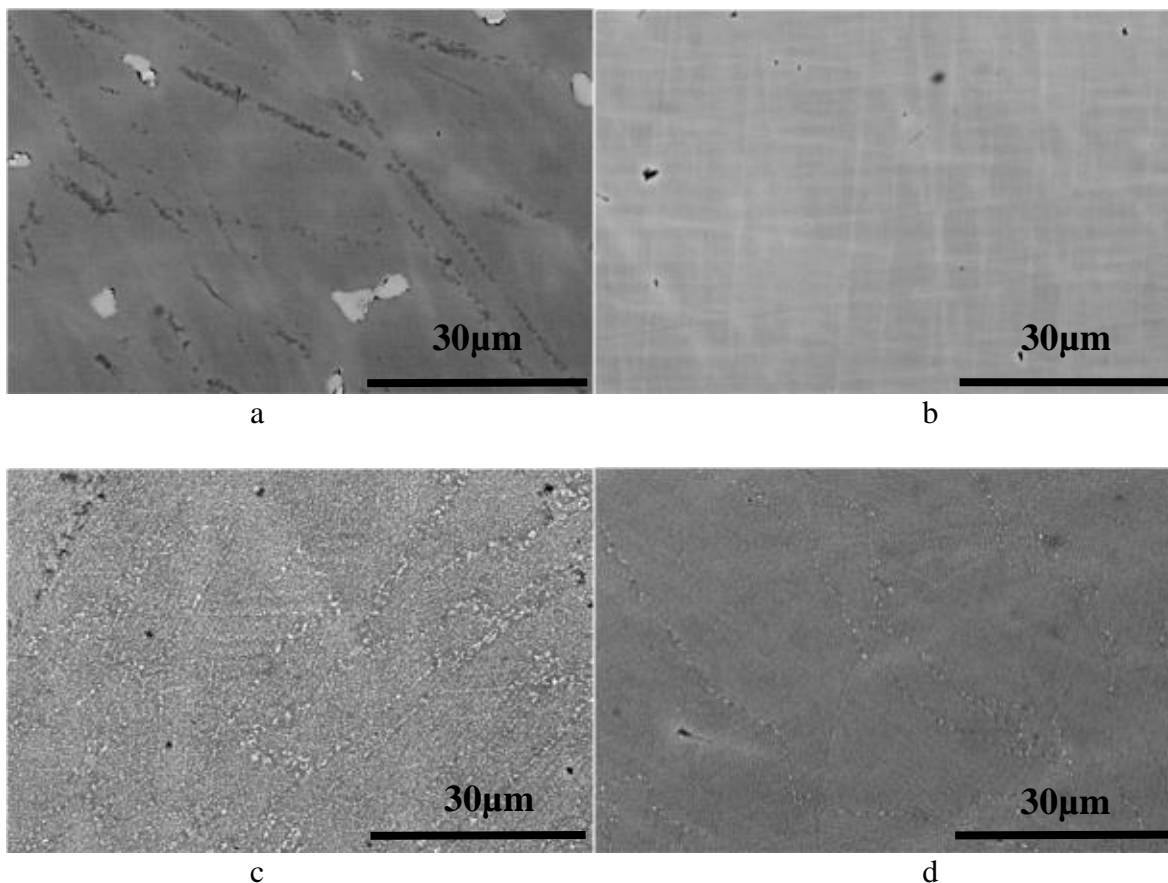


Figure 7. i - t plots recorded for all four studied samples at +250 mV vs. E_{Corr} , 37⁰C and 15 min.

The sample obtained by the CAS technology exhibits the lowest residual current after 15 minutes at the given potential, followed closely by the probe obtained by CAD milling.



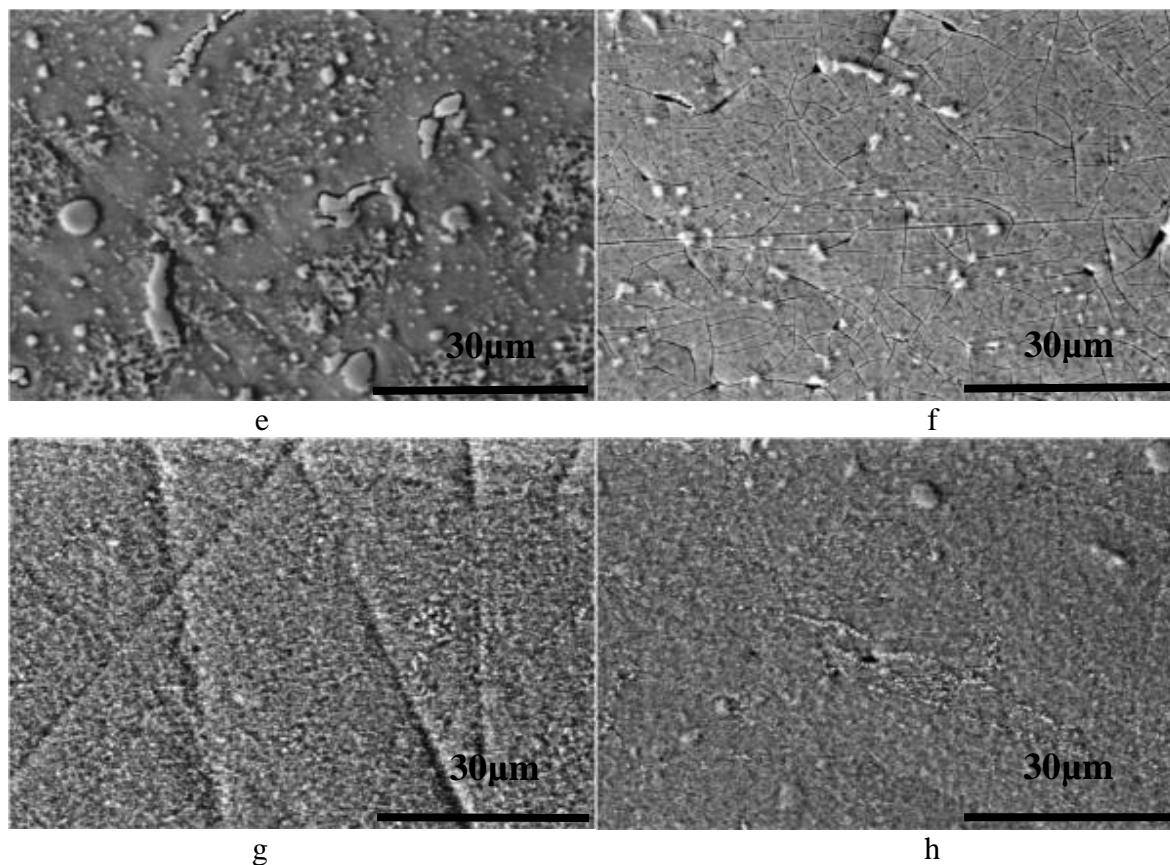


Figure 8. SEM micrographs of samples obtained by a-e CAS; b-f MIL; c-g SLM and d-h SLS before and after corrosion testing in artificial saliva at 37⁰C, 30 μm scale.

This factor denotes a relatively high degree of protection against electrochemical corrosion provided by the oxide layer that may be formed on the metal surface, in accordance to literature data [25].

Surface analysis was performed in order to further characterize the obtained alloy samples with respect to the modification of the surface morphology after corrosion testing.

Metallographic surface analysis of the alloys prepared through various processing technologies has been undertaken by means of SEM, in order to distinguish corrosion or pitting sites along the exposed metallic surface. After performing corrosion testing the surfaces of CAS as well as that of MIL are characterized by a grain boundary phase grown onto the primary homogenous surface structure (Figure 8 a, e and b, f), the first exhibiting pseudo dendritic character. Samples obtained by SLM and SLS exhibit mostly a dendritic surface morphology with very little graining observed on the surface of SLM after corrosion testing, while the SLS probe shows some graining effects.

Processing technology has been shown to have significant influence on the microstructure and surface morphology of the studied probes [21, 26]. Roughness and surface characteristics can alter the corrosion behaviour of metallic structures [2]. Casting technology itself influences piece quality, with casting defects, micro-cracks, dendritic structures, leading to a higher tendency of metal dissolution, i.e. metal ion release. [27,28]. MIL exhibit the best structural characteristics, SLS and SLM present

internal and surface pores due to the employed technology, while CAS show numerous inclusions, higher porosity and metal oxides formed during melting and casting [29].

Corrosion resistance is most probably provided by the formation of a passive oxide layer when the alloy is in contact with atmospheric oxygen. Although in the studied dental alloys cobalt is predominant, previous researches indicates that it can be found in relatively small amounts in the formed oxide layer coatings [5]. In consequence, changes in the composition or in the microstructure of the base alloy can lead to major changes in the morphology and chemistry of the formed passivating oxide layer, hence dramatically affecting the biocompatibility of the employed alloys [26].

4. CONCLUSIONS

Computer assisted processing technologies of dental alloys showed promising results from the electrochemical point of view, representing a good alternative to traditional manufacturing methods for metallic frameworks of dental prostheses.

A passivating oxide layer probably formed on the metal surface of all the tested alloys provides a high degree of protection against electrochemical corrosion observed on the whole array of investigated samples.

The Co-Cr frameworks processed by computer aided technologies are characterized by a relatively high corrosion resistance similar to that of conventional obtained samples.

Differences in the electrochemical behaviour can be attributed to the microstructure and surface morphology, which can be improved especially for SLS and SLM technologies by optimizing the process parameters.

References

1. Y. Pan, L. Jiang, H. Lin and H. Cheng, *Dent. Mater. J.*, 36 (2017) 82.
2. H.R. Kim, Y.K. Kim, J.S. Son, B.Y. Min, K.H. Kim and T.Y. Kwon, *Mater. Lett.*, 178 (2016) 300.
3. M.A. Bortagaray, C.A.A. Ibañez, M.C. Ibañez and J.C. Ibañez, *Open. Dent. J.*, 10 (2016) 486.
4. C. Lu, Y. Zheng and Q. Zhong, *PLOS ONE.*, 12 (2017) e0174440.
5. X.Z. Xin, J. Chen, N. Xiang, Y. Gong and B. Wei, *Dent. Mater.*, 30 (2014) 263.
6. L. Porojan, C.E. Savencu, L.V. Costea, M.L. Dan, S.D. Porojan, *Int. J. Electrochem. Sci.*, 13 (2018) 410
7. S.K. Santos, R.F. Jaimes, S.O. Rogero, P.A. Nascente and S.M. Agostinho, *Braz. Dent. J.*, 27 (2016) 181.
8. S.I. Drob, C. Vasilescu, M. Andrei, J.M. Calderon Moreno, I. Demetrescu and E. Vasilescu, *Mater. Corros.*, 67 (2016) 739.
9. J. Nierlich, S.N. Papageorgiou, C. Bourauel, R. Hültenschmidt, S. Bayer, H. Stark and L. Keilig, *E.J.O.S.*, 124 (2016) 287.
10. V.J. Pulikkottil, S. Chidambaram, P.U. Bejoy, P.K. Femin, P. Paul and M. Rishad, *J. Pharm. Bioall. Sci.*, 8 (2016) S96.
11. Y. Al Jabbari, A. Ntasi, M. Gaintatzopoulou, W.D. Mueller, G. Eliades, E-S. M. Sherif and S. Zinelis, *Int. J. Electrochem. Sci.*, 11 (2016) 2982.

12. International Organization for Standardization ISO 10271, Dental metallic materials- Corrosion test methods, Berlin Wien Zurich:Beuth Verlag GmbH, 2001.
13. G.J. Gerstorfer and H. Weber, *Dtsch. Zahnärztl.*, 40 (1985) 87.
14. M.C. Lucchetti, G. Fratto, F. Valeriani, E. De Vittori, S. Giampaoli, P. Papetti, V. Romano Spica and L. Manzon, *J. Prosthetic. Dent.*, 114 (2015) 602.
15. A. Milheiro, K. Nozaki, C.J. Kleverlaan, J. Muris, H. Miura and A.J. Feilzer, *Odontology*, 104 (2016) 136.
16. J.R. Pontes, A.C. Alves, F. Toptan, R. Galo and E. Ariza, *Mat. Corr.*, 67 (2016) 306.
17. D.M. Sarantopoulos, K.A. Beck, R. Holsen and D.W. Berzins, *J. Prosthet. Dent.*, 105 (2011) 35.
18. W.J. Silva, L.L. Sousa, R.Z. Nakazato, E.N. Codaro and H. de Felipe, *Mat. Sci. Appl.*, 2 (2011) 42.
19. B. Galateanu, F. Golgovici, A. Hudita, M. Stan, S. Dinescu, M. Costache, I. Demetrescu and A. Popescu, *Mat. Corr.*, 67 (2016) 1096.
20. P.P. Ming, S. Shao, J. Qiu, Y. Yu, J. Chen, J. Yang, W. Zhu, M. Li and C. Tan, *R.S.C. Adv.*, 7 (2017) 5843.
21. S. Capelo, L. Proença, J.C.S. Fernandes and I.T.E. Fonseca, *Int. J. Electrochem. Sci.*, 9 (2014) 593.
22. F. Marken, A. Neudeck, A.M. Bond, Cyclic Voltammetry, In: F. Scholz, editor, *Electroanalytical Methods, Guide to Experiments and Applications*, Springer-Verlag Berlin Heidelberg, p. 83-85 (2010).
23. V.S. Saji and H.C. Choe, *Trans. Nonferrous Met. Soc. China*, 19 (2009) 785.
24. I. Diaz, J.F. Martinez-Lerma, R. Montoya, I. Llorente, M.L. Escudero, M.C. García-Alonso, *Bioelectrochem.*, 115 (2017) 1.
25. X-Z. Xin, J. Chen, N. Xiang, Y. Gong and B. Wei, *Dent. Mater. J.*, 30 (2014) 263.
26. Y.S. Hedberg, B. Qian, Z. Shen, S. Virtanen and I.O. Wallinder, *Dent. Mater. J.*, 30 (2014) 525.
27. L. Porojan, M. Birdeanu, C. Savencu and S. Porojan, *Rev. Chim.*, 11 (2017) 2538.
28. R. Galo, L.A. Rocha, A.C. Faria, R.R. Silveira, R.F. Ribeiro and de M.G.C. Mattos, *Mater. Sci. Eng. C.*, 45 (2014) 519.
29. L. Porojan, S. Porojan, C. Bortun and C.E. Savencu, *Rev. Chim.*, 66 (2015) 210.